

## Supplementary data for

### Self-assembly of gold nanowire networks into gold foams: production, ultrastructure and applications.

Anshuman Jakhmola<sup>a,†</sup>, Maurizio Celentano<sup>b,†</sup>, Raffaele Vecchione<sup>a,b\*</sup>, Anastasios Manikas<sup>a</sup>, Edmondo Battista<sup>a,b</sup>, Vincenzo Calcagno<sup>a,b</sup>, Paolo A. Netti<sup>a,b</sup>

† These authors contributed equally to the work

**Fig. S1.** (a) SEM micrograph (b) EDS elemental microanalysis of gold foam-TB(c) EDS spectra of pure gold foam displaying gold peak together with peaks of carbon and silica originating from citrate and silica wafer substrate.

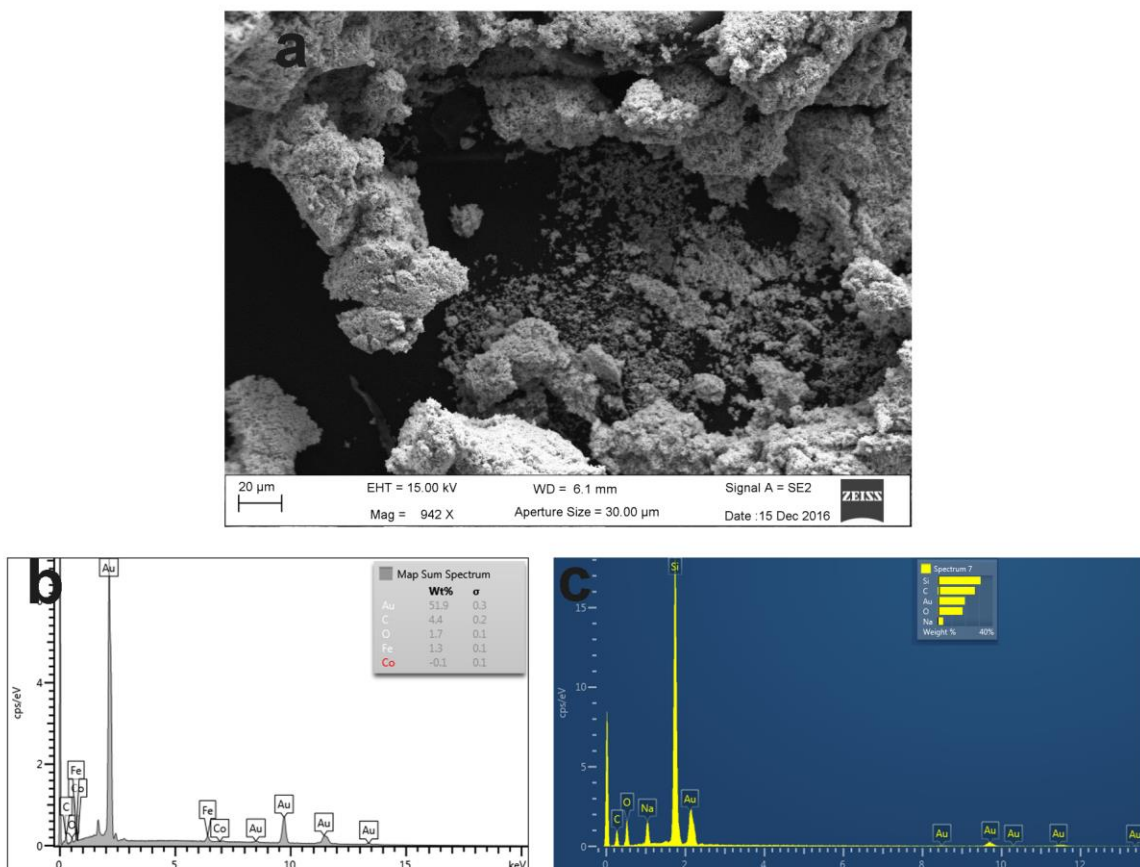


**Fig. S2:** Confocal image displaying encapsulation of heat labile biomolecule (antibody) in the pores and cavities of gold foam ( $R=9.7$ ).

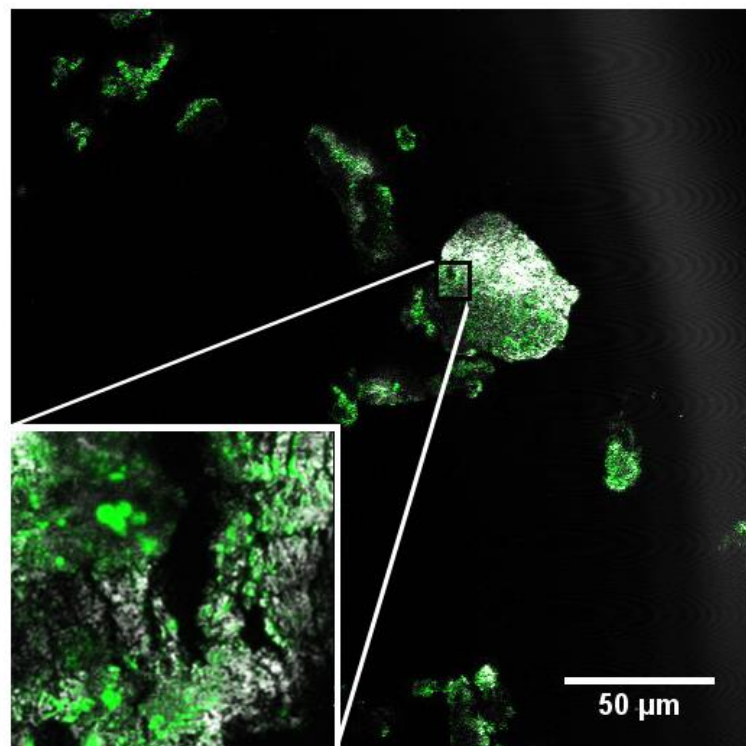
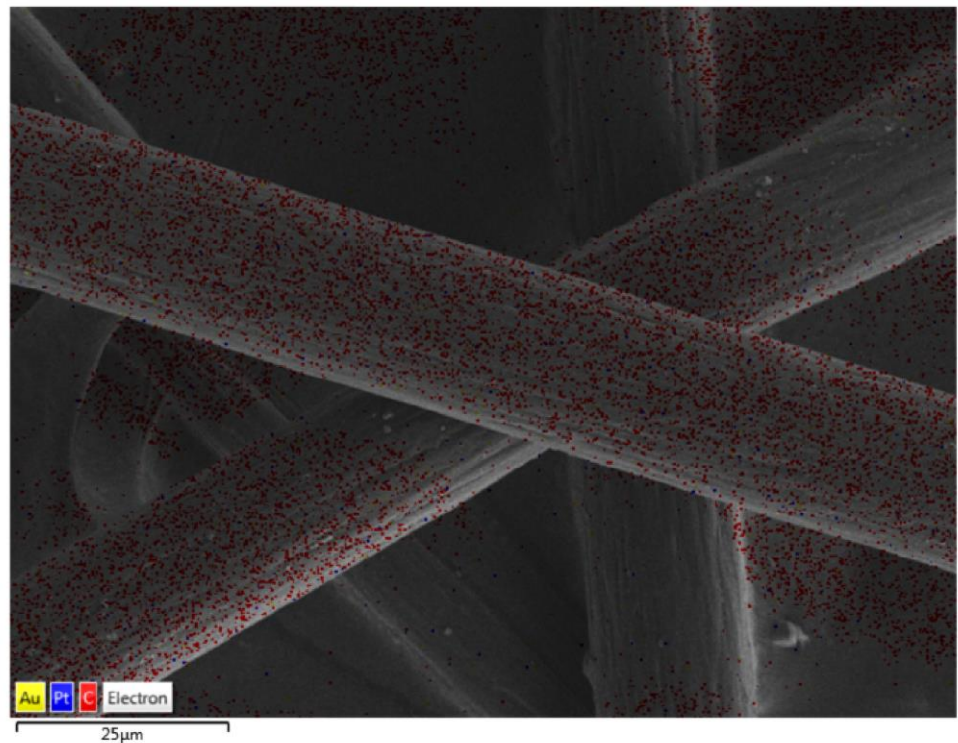


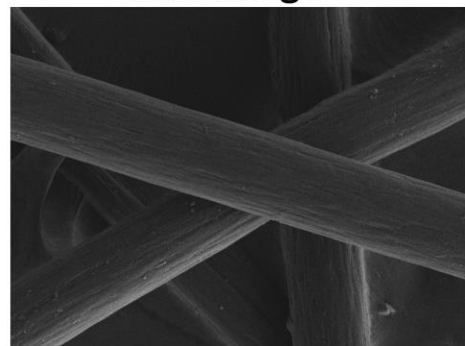
**Fig. S3.** SEM images and EDS elemental maps of (a) commercial cotton fibers and (b) commercial cotton fibers coated with gold foams. Metal sputtering (Pt/Pd) was necessary to observe the cotton samples therefore signal from cotton (C atoms) and metal coating (Pt/Pd) were detected. Signals from Au were also detected but they were very less intense. EDS elemental mapping of magnetically cotton fibers treated with magnetically responsive gold foams showed clearly a compact coating of gold foams with magnetic nanoparticles embedded in them.

a)

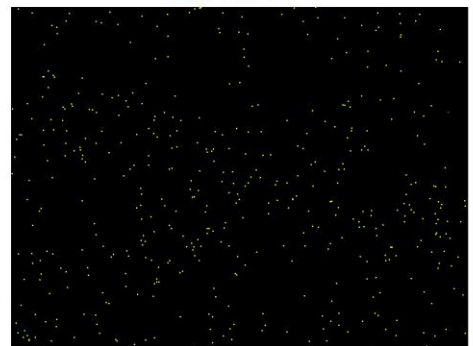
EDS Layered Image



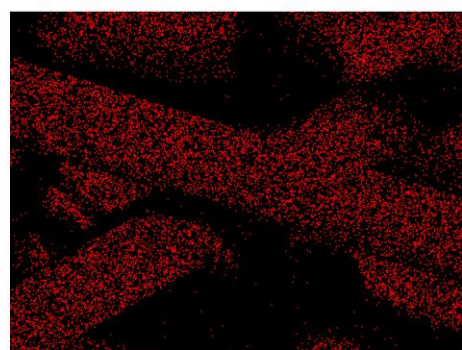
SEM Image



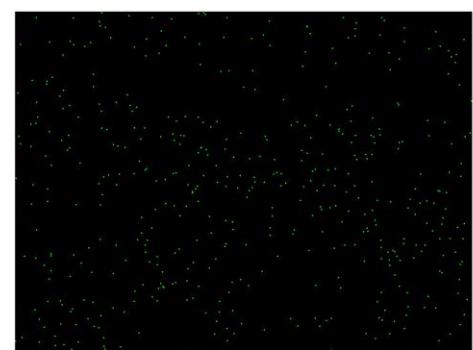
Au M $\alpha$ 1



C K $\alpha$  1\_2

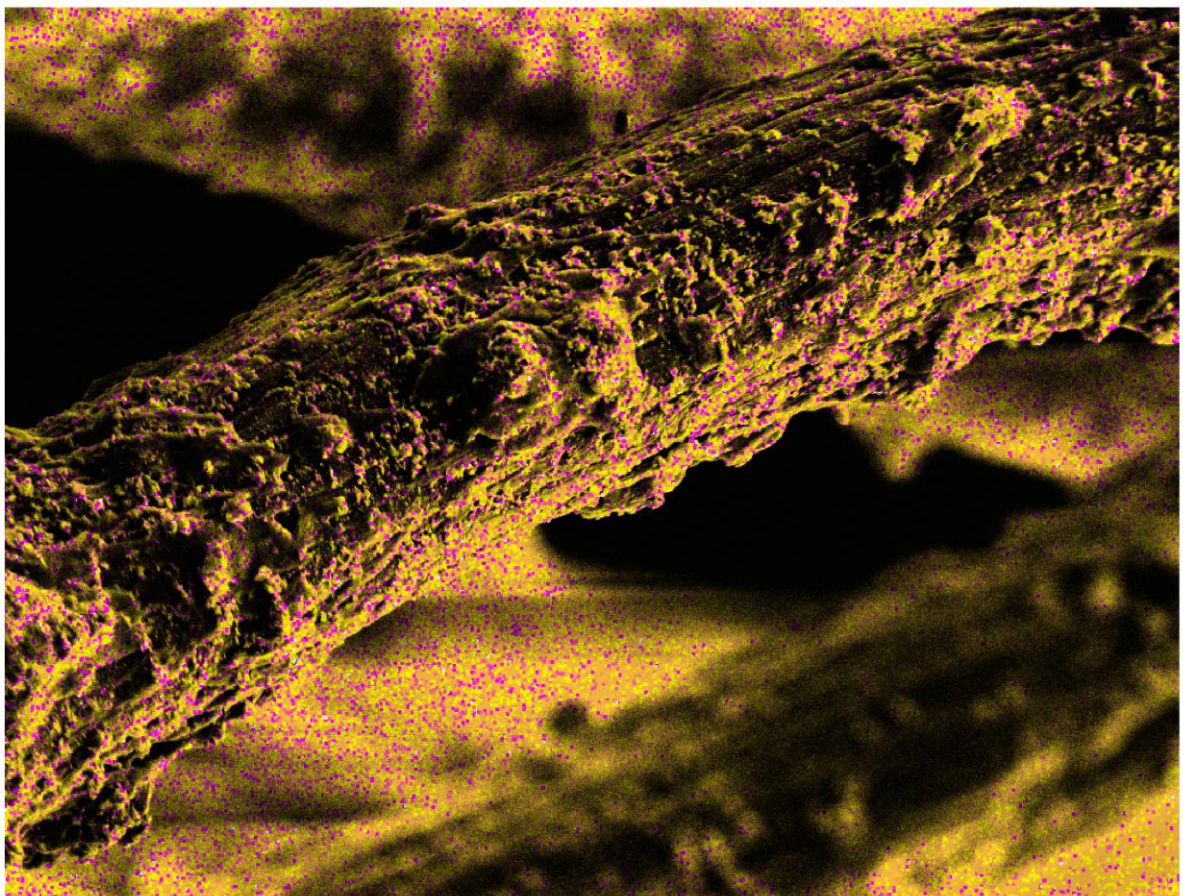


Pt M $\alpha$ 1

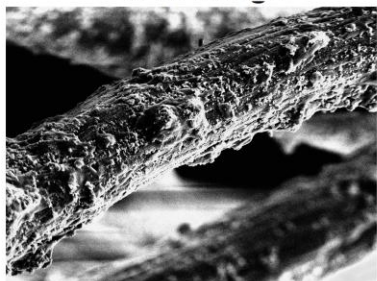


**b)**

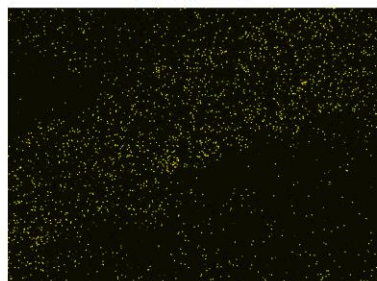
**EDS Layered Image**



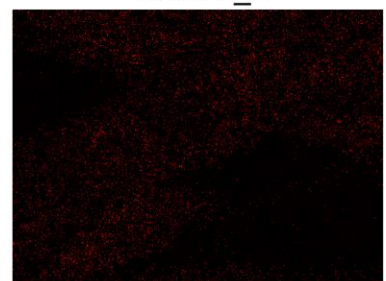
**SEM Image**



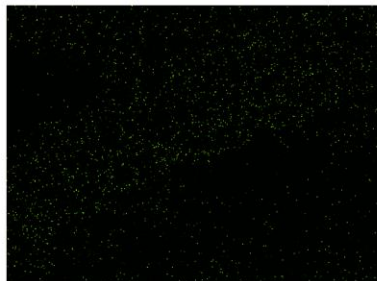
**Au M $\alpha$ 1**



**C K $\alpha$  1\_2**



**Pt M $\alpha$ 1**



**Fe L series**



**Fig. S4.** TEM micrographs and SAED pattern at  $R = 19.4$  displaying almost homogeneous diameters of individual nanowires and their polycrystalline crystal structure. (d) High magnification micrograph displaying formation of head/islands by merging of nanoparticles of different lattice orientations

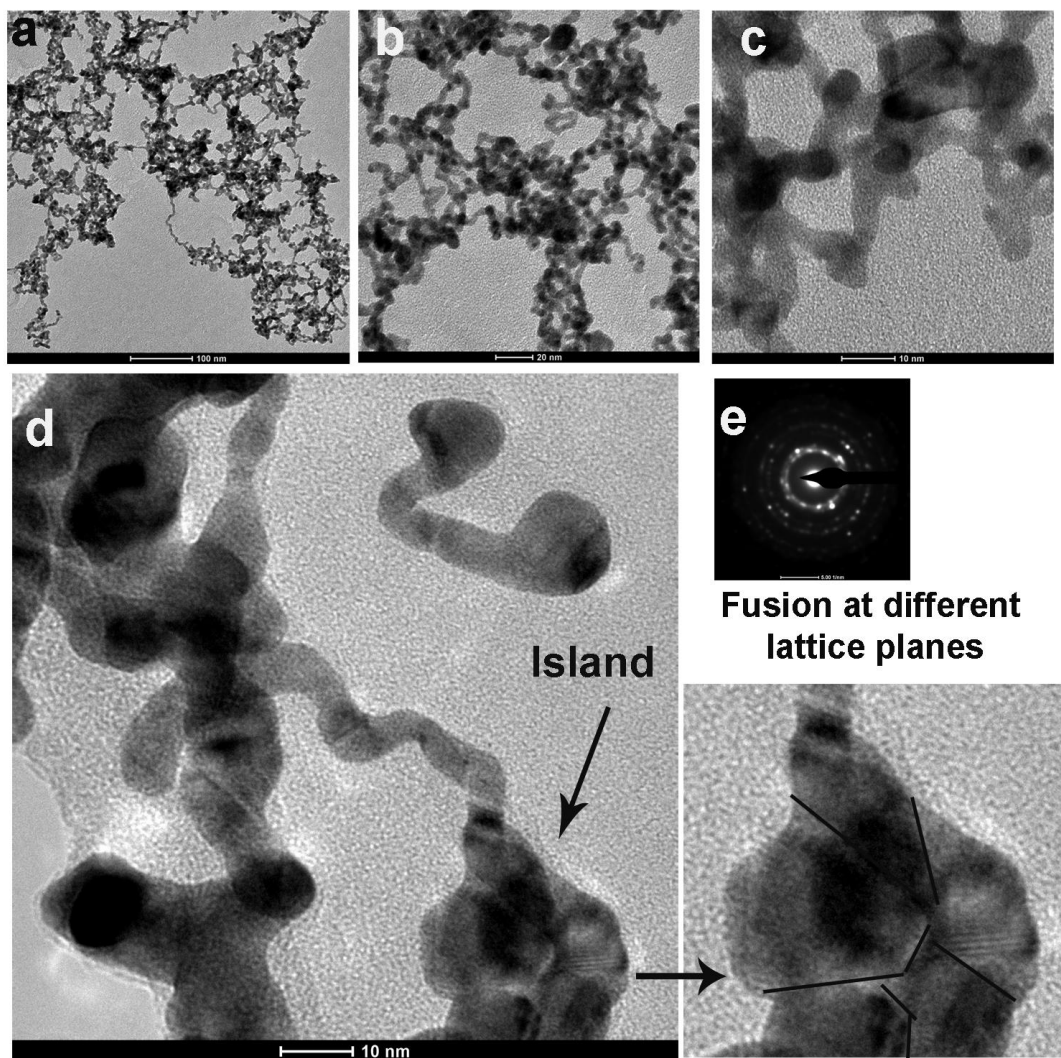


**Fig. S5.** TEM micrograph at  $R = 6$  displaying mixture of irregular particles.

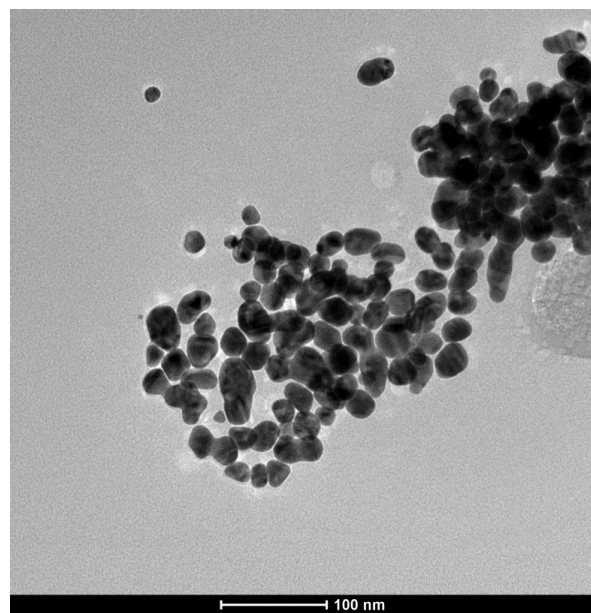
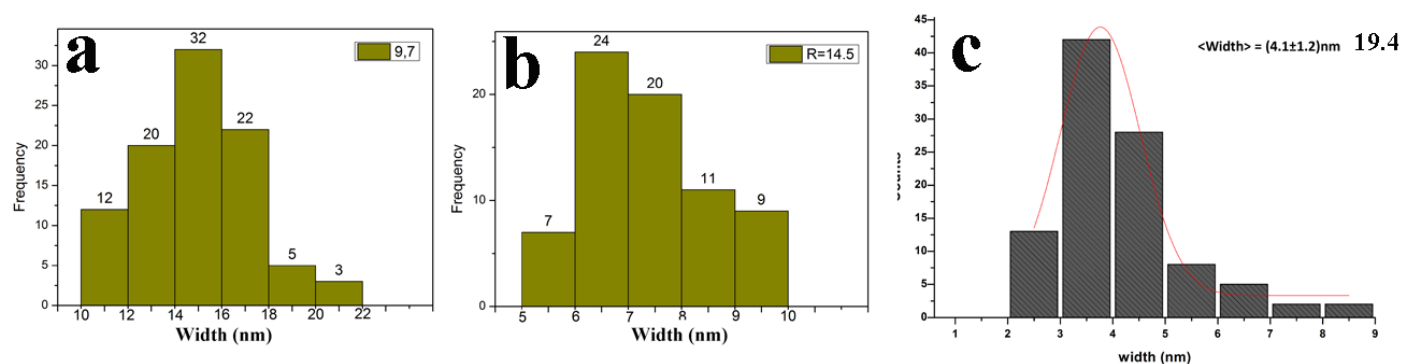


**Fig. S6.** Size histograms of NWNs at  $R =$  (a) 9.7; (b) 14.55 and (c) 19.4



## UV-Vis and Kinetic studies

The ability of citrate to reduce  $\text{Au}^{3+}$  ions at room temperature was initially studied by UV-vis spectroscopy. In this study the amount of  $\text{Au}^{3+}$  was kept constant and the amount of citrate was gradually increased. On varying R between 7.3 and above (till 19.4 and even higher) the solutions were either blackish or blue black in appearance and displayed flat absorption profiles from 500 to 800 nm indicating absorption of photons of all energies. The broad spectrum and black color of colloidal solution indicated anisotropic growth and are due to superposition of longitudinal resonance of different aspect ratio gold nanowires of variable length, a phenomenon generally observed in NWN type structures [1,2]. After initial mixing of citrate and gold solutions an induction period was observed (Supporting Table S1) which was marked with the presence of peaks originating from reactants only (chloroauric ions and citrate) [3]. The induction period was followed by nucleation and growth of the particles during which the solution became nearly colorless. This was followed by a broad plasmon band and increase in absorbance in the entire visible–NIR region with a prominent isosbestic point at around 250 nm (Supporting Fig. S4). The increase in absorbance in the entire wavelength range could be attributed to the formation and growth of the nanowires and denser network structure with time. A careful look at the final UV-vis spectra of all the R values above 7.3 shows minute differences, e.g. broad peak at 550 nm becomes more flattened on increasing the R, likely due to more uniformity in the structure.

**Fig. S7.** Kinetics of the formation of gold nanoparticles at different citrate to gold ratio (R from 7.3 to 19.4 = NWNs).

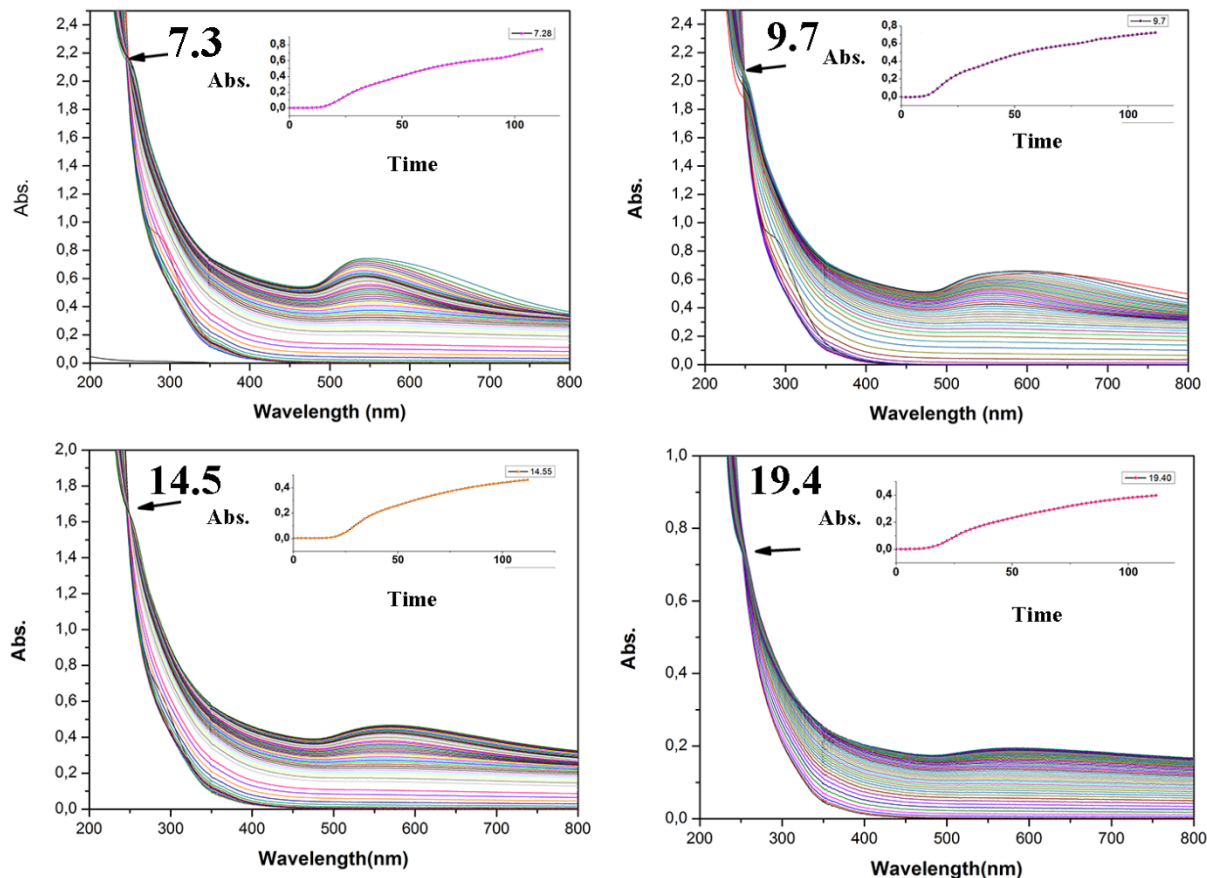


**Table S1.** Induction time for all samples as measured from UV/visible spectroscopy.

Ratio	Induction Time (min.)
7.3	12
9.7	11
14.85	14
19.4	10

## XPS analysis

### Experimental

X-Ray Photoelectron spectra were recorded on a XPS Versa Probe II (PHI, Chanhassen US) by large area analysis mode where the monochromatic Al anodic beam of 100  $\mu\text{m}$ , at 100 W power, normal to the surface, is rastered over an area of  $1400 \times 300 \mu\text{m}$  with the analyzer fixed at  $45^\circ$  with sample surface. Survey spectra were acquired with an accumulation time of at least 20 min at high pass energy (187 KeV) while high resolution spectra of the elements of interest were acquired at a pass energy of 11.7 KeV with same power as above and at 0.1 eV resolution. Spectra were analyzed by Multipack (PHI, Chanhassen US) software and all the peaks were referenced to the adventitious carbon peaks C1s at 284.8 eV binding energy. Together with carbon, oxygen, nitrogen and gold other elements are also present, such as sodium (Na 1s, 1071 eV and Auger peaks at 497 eV) and silicon (Si 2s and 2p at 150 eV and 97 eV), but not quantified in the analysis as considered contaminants mainly due to the substrate where we drop casted the nanoparticles. Samples were prepared by dropping a suspension of the gold nanoparticles on a flat surface of silicon and the liquid evaporated in a vacuum chamber. As controls raw materials as well as the suspending media after several washes of nanoparticles were also analyzed (Data not shown).

## XPS analysis

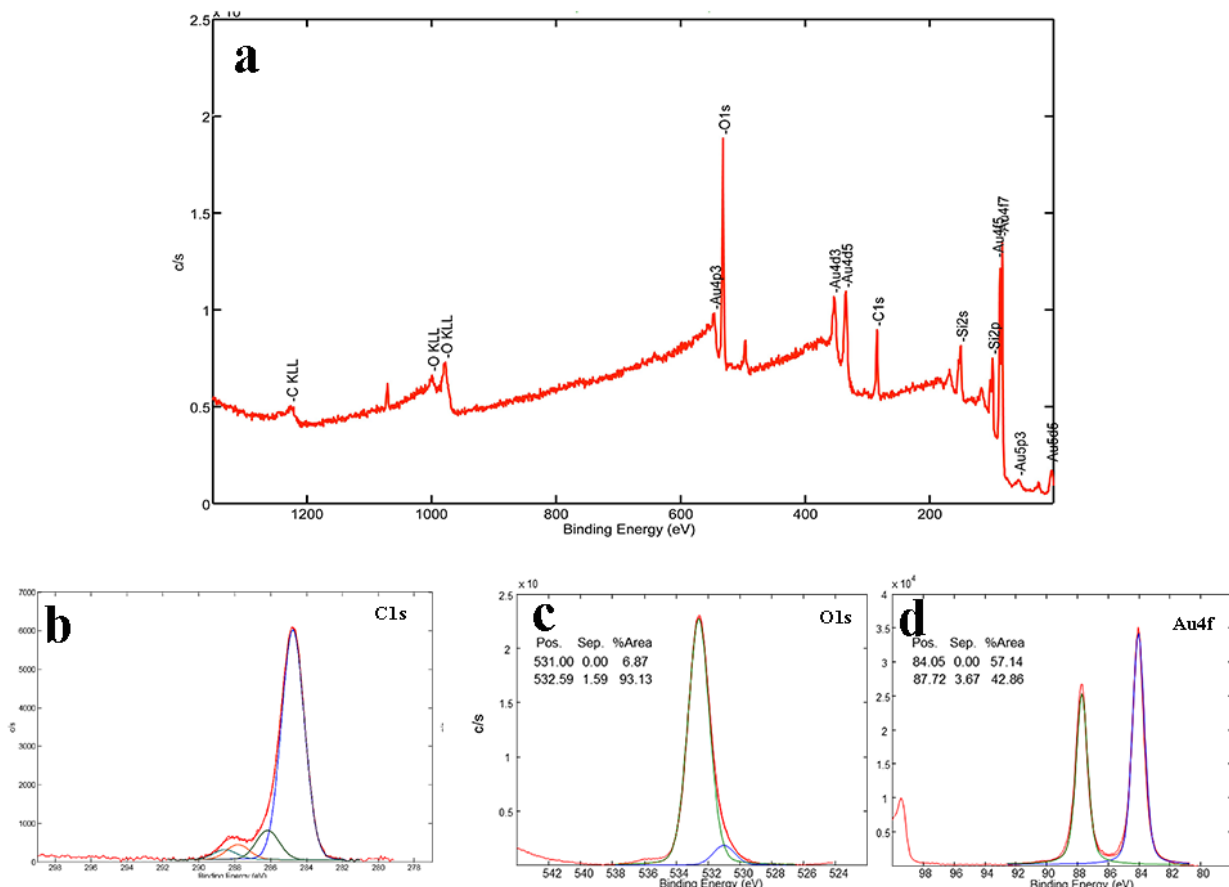
To further probe into the structure of the nanowires we carried out XPS analysis of gold NWNs. The XPS results (survey spectra) show that the NWNs are made up of pure metallic gold, which can be confirmed from the binding energy for Au 4f7/2 located at 84 eVs. Notably peaks corresponding to oxygen, carbon, were also seen with Au signals which were due to citrate on the surface of particles (Fig. S5a). Table S2 reports all the assignments and the relative elemental quantification after fitting by Gaussian deconvolution- the peaks of each core line. Gold NWNs

synthesized at  $R = 9.7$  were taken as reference material and the carbon 1s (C1s) was fitted with four peaks corresponding to (i) adventitious and aliphatic hydrocarbons at 284.8 eV, (ii) C-OH at 286.16 eV, (iii) carboxyl groups coordinated with Au atoms (COO-Au) at 287.82 eV, (iv) free carboxyl groups (COOH) at 288.52 eV (Fig. S5b). This assignment is in agreement with the work of Shumaker-Parry [4] where they found specific ionic type interaction between gold and carboxyl groups (peak at 287.82 eV). Further analysis of O1s core lines can be deconvoluted in two peaks: 532.59 and 531 eV, respectively attributed to oxygen of carboxyl and alcohol and to the oxygen in close proximity to electron donating species like  $\text{Au}^0$  (Fig. S5c) [5]. However, the absence of peaks attributable to Au-O binding in the Au core line ( $\text{Au } f_{5/2} 84.05$  eV) [4] suggests that in our samples the interaction between the gold surface and the citrate takes place through the formation of Au-CO  $\pi$  back bond.

**Table S2.** XPS chemical shifts, assignments and relative elemental surface concentrations; precision in the binding energies were 0,1 eV after at least three independent acquisitions.

cit-AuNNWs				
core lines		B.E.(eV) at %		
C1s	C-C	284.80	29.3	
	C-OH	286.16	3.63	
	COO-Au	287.82	1.87	
	COOH	288.52	1.27	
O1s	O-C=O-Au	531	3.85	
	O-C=O/C-OH	532.59	52.14	
Au4f	4f <sub>5/2</sub>	84.05		7.94
	4f <sub>7/2</sub>	87.72		

**Fig. S8.** XPS spectra of nanowire networks (a) Survey spectrum of the NWNs with the elemental composition. The silicon Si2s and the related signals are coming from the substrate where the nanoparticles were deposited. High resolution XPS for carbon (b) C1s, (c) O1s and (d) Au4f peak for NWNs.

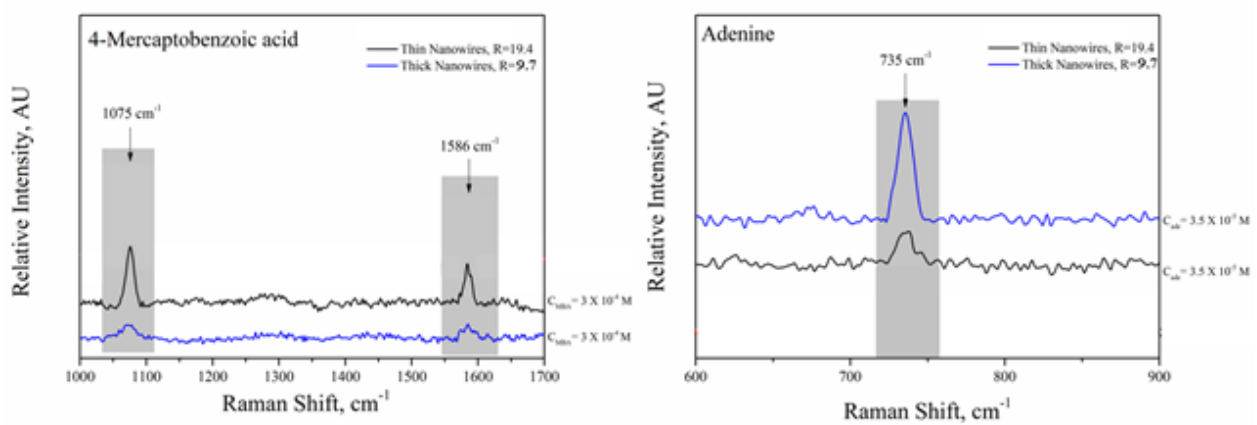


### SERS experiments on the nanowire networks (NWNs at R 9.7 and 19.4)

SERS experiments on both thick and thin gold NWNs were carried out. Adenine and 4-MBA were used as probe molecules and have been widely used in SERS experiments because both of them adsorb firmly on gold surface (adenine *via* the amine group and 4-MBA via the sulphur containing on to the mercapto group) [6,7]. For nanowires we chose two representative examples

the thick one with diameters around 15 nm ( $R = 9.7$ ) and the thin one with diameters around 4 nm ( $R = 19.4$ ). As it is shown from the Fig. S9 both thick and thin NWNs generate SERS spectra with a significant enhancement to the Raman scattering. In both cases it was possible to record the spectra of adenine and 4-MBA at a concentration of  $3.5 \times 10^{-5}$  M and  $3 \times 10^{-4}$  M respectively while the enhancement factor was found to be around  $10^4$ . The characteristic bands for both adenine and 4-MBA are also presented in Fig. S9. The band, at  $735 \text{ cm}^{-1}$  is the characteristic Raman band of adenine assigned to the ring breathing mode while 4-MBA displayed characteristic bands at 1075 and  $1586 \text{ cm}^{-1}$  assigned to the ring stretching and breathing mode respectively. In summary, the anisotropic particles showed a significant enhancement in the Raman scattering of the probe molecules adenine and MBA and can be easily used as SERS active substrates. Taking in account also that the synthetic procedure is much simpler than the classical ones their usage can be adopted for more SERS applications.

**Fig. S9.** SERS spectra of adenine and 4-MBA on, thick nanowires  $R=9.7$  and thin nanowires  $R=19.4$ ).



## References

1. L. Pei, K. Mori, M. Adachi, Formation process of two-dimensional networked gold nanowires by citrate reduction of  $\text{AuCl}^4^-$  and the Shape Stabilization. *Langmuir* 20 (2004) 7837-7843.
2. B.-K Pong, H. I. Elim, J.-X. Chong, W. Ji, B. L. Trout, J.-Y. Lee, New insights on the nanoparticle growth mechanism in the citrate reduction of Gold(III) salt: Formation of the Au nanowire intermediate and its nonlinear optical properties. *J. Phys. Chem. C* 111 (2007) 6281-6287.
3. M. Wuithschick, A. Birnbaum, S. Witte, M. Sztucki, U. Vainio, N. Pinna, K. Rademann, F. Emmerling, R. Krahnert, J. Polte, Turkevich in new robes: Key questions answered for the most common gold nanoparticle synthesis. *ACS Nano* 9 (2015) 7052-7071.
4. J. -W. Park, J. S. Shumaker-Parry, Structural study of citrate layers on gold nanoparticles: Role of intermolecular Iinteractions in stabilizing nanoparticles. *J. Am. Chem. Soc.* 136 (2014) 1907-1921.
5. A. Patnaik, C. Li, Evidence for metal interaction in gold metallized polycarbonate films: An X-ray photoelectron spectroscopy investigation. *J. Appl. Phys.* 83 (1998) 3049-3056
6. A. C. Manikas, A. Papa, F. Causa, G. Romeo, P. A. Netti, Bimetallic Au/Ag nanoparticle loading on PNIPAAm–VAA–CS8 thermoresponsive hydrogel surfaces using ss-DNA coupling, and their SERS efficiency. *RSC Adv.* 5 (2015) 13507-13512.
7. S. Schlücker, S. Surface-enhanced raman spectroscopy: Concepts and chemical applications. *Angew. Chem. Int. Ed.* 53 (2014) 4756-4795.